

Nuclear pairing from chiral pion-nucleon dynamics: Applications to finite nuclei

Paolo Finelli

Physics Department, University of Bologna, I-40126 Bologna, Italy INFN, Bologna Section, I-40126 Bologna, Italy

Tamara Nikšić and Dario Vretenar

Physics Department, Faculty of Science, University of Zagreb, HR-10000 Zagreb, Croatia

(Received 22 November 2011; revised manuscript received 25 July 2012; published 19 September 2012)

The 1S_0 pairing gap in isospin-symmetric nuclear matter and finite nuclei is investigated using the chiral nucleon-nucleon potential at the next-to-next-to-next-to-leading order (N^3LO) order in the two-body sector and the next-to-next-to-leading order (N^2LO) order in the three-body sector. To include realistic nuclear forces in the relativistic Hartree-Bogoliubov (RHB) framework, we employ a separable form of the pairing interaction that is adjusted to the nuclear matter pairing gap computed with a bare nuclear force. The separable pairing force is applied to the analysis of pairing properties for several isotopic and isotonic chains of spherical nuclei.

DOI: [10.1103/PhysRevC.86.034327](https://doi.org/10.1103/PhysRevC.86.034327)

PACS number(s): 21.30.-x, 74.20.Rp, 21.10.Dr, 21.60.Jz

I. INTRODUCTION

Nuclear energy density functionals (EDF) provide a microscopic, globally accurate, and yet economic description of ground-state properties and collective excitations over the whole nuclide chart. Even though it originates in the effective interaction between nucleons, a generic density functional is not necessarily related to any given nucleon-nucleon (NN) potential and, in fact, some of the most successful modern functionals are entirely empirical [1]. Of course, it is very desirable to have a fully microscopic foundation for a universal density functional, and this is certainly one of the major challenges in low-energy nuclear structure physics [2].

The EDF approach to nuclear structure is analogous to Kohn-Sham density functional theory (DFT) and, because it includes correlations, goes beyond the Hartree-Fock approximation. Kohn-Sham DFT has the advantage of being a local scheme, but its usefulness crucially depends on our ability to construct accurate approximations for the most important part of the functional, that is, the universal exchange-correlation functional [3].

In a series of recent articles [4–6] concepts of effective field theory and DFT have been used to derive a microscopic relativistic EDF-based model of nuclear many-body dynamics constrained by in-medium QCD sum rules and chiral symmetry. The density dependence of the effective nucleon-nucleon couplings in this model (called FKVW in the following) is determined from the long- and intermediate-range interactions generated by one- and two-pion exchange processes. They are computed using in-medium chiral perturbation theory, explicitly including $\Delta(1232)$ degrees of freedom [7]. Divergent contributions to the nuclear matter energy density, calculated at the three-loop level, are absorbed by a few contact terms. These constants are understood to encode unresolved short-distance dynamics.

The relativistic FKVW model has been employed in studies of ground-state properties of spherical and deformed nuclei using the relativistic Hartree-Bogoliubov framework (RHB [8]). In the description of open-shell nuclei, in particular, a hybrid model has been used with the FKVW Kohn-Sham potential in the particle-hole (ph) channel and, like in most

applications of RHB-based models, the pairing part of the empirical Gogny force [9] in the particle-particle (pp) channel.

Even though this approach has been very successful, it is not theoretically consistent because of the choice of the empirical effective interaction in the pp channel. As an important part of a larger program to develop a framework of fully microscopic nuclear energy density functionals, much effort has recently been devoted to designing nonempirical pairing functionals [10–14].

The aim of this work is to formulate a consistent microscopic framework for open-shell nuclei, in which both the ph and the pp channels of the effective internucleon interaction are determined by chiral pion-nucleon dynamics. Thus we consider a separable pp interaction based on a microscopic pairing interaction constrained by chiral dynamics (see Ref. [15] for previous calculations involving the next-to-next-to-leading order [N^2LO] chiral potential), combine it with the FKVW functional in the ph channel, and, employing the corresponding RHB model, present a study of pairing gaps in isotopic and isotonic chains of spherical open-shell nuclei.

We use the realistic NN potential developed by the Idaho group at next-to-next-to-next-to-leading order (N^3LO) in the chiral expansion [16] (see also Ref. [17]), and a two-body density-dependent potential derived from the relevant diagrams at the N^2LO order in the three-body sector [18] (see also Refs. [14,19–22] for similar approaches and pertinent details).

The paper is organized as follows. In Sec. II we discuss results for the pairing gap of nuclear matter in the BCS approximation. Section III briefly reviews the method introduced by Duguet [10,23], and later by Tian *et al.* [24,25], to apply realistic pairing interactions to calculations of finite nuclei. In Sec. IV we analyze pairing gaps in spherical nuclei for several isotopic and isotonic chains. Section V summarizes the principal results.

II. PAIRING GAP IN A HOMOGENEOUS INFINITE SYSTEM

The momentum and density-dependent pairing field $\Delta(k, k_F)$ in infinite matter is determined by the solution of

the BCS gap equation

$$\Delta(k, k_F) = -\frac{1}{4\pi^2} \int_0^\infty \frac{p^2 V(p, k) \Delta(p, k_F)}{\sqrt{[\mathcal{E}(p, k_F) - \mathcal{E}(k_F, k_F)]^2 + \Delta(p, k_F)^2}} dp, \quad (1)$$

where $V(p, k)$ represents the off-shell pairing potential in momentum space, $\mathcal{E}(p, k_F)$ is the in-medium single-particle energy, and $\mathcal{E}(k_F, k_F)$ is the Fermi energy.

The effective force in the pairing channel is, in principle, generated by the sum of all particle-particle irreducible Feynman diagrams [26]. In most application to nuclear and neutron matter, however, only the lowest-order term, which corresponds to the bare nucleon-nucleon interaction, is retained [27]. Terms of higher order in the effective pairing interaction represent screening corrections to the bare force, caused by medium polarization effects (see Refs. [28,29] and references therein). In the present analysis we consider only the bare interaction, while a study of polarization effects will be carried out in a forthcoming paper.

For the pairing potential $V(p, k)$ we employ the simple ansatz

$$V(p, k) = V_{2B}(p, k) + V_{3B}(p, k, m) \simeq V_{2B}(p, k) + \bar{V}_{2B}(k_F, p, k), \quad (2)$$

where the three-body potential is approximated by an effective two-body density-dependent potential \bar{V}_{2B} derived by Holt *et al.* in Ref. [18]. These authors showed that in the singlet channel (1S_0) the overall effect of $\bar{V}_{2B}(k_F, p, k)$ is to reduce the strong S -wave attraction (cf. Fig. 6 of Ref. [18]). As suggested in Ref. [18], here we neglect a possible isotopic dependence that, in any case, is expected to be rather small for the nuclei considered in the present analysis (see also Ref. [14]). For both terms in Eq. (2) we follow standard procedures for the regulator functions and refer the reader to the original papers for details.

For the single-particle spectrum that appears in the denominator of the gap equation (1) we employ the simple quadratic form

$$\mathcal{E}(p, k_F) - \mathcal{E}(k_F, k_F) = \frac{p^2 - k_F^2}{2M^*(k_F)}. \quad (3)$$

This approximation should suffice because the momenta p around k_F give the dominant contribution to the integral in Eq. (1). The effective nucleon mass $M^*(k_F)$ was obtained in a very recent calculation (Fig. 9 of Ref. [30]), in which the nuclear energy density functional was derived to first order in the two- and three-nucleon interactions using a density matrix expansion.¹

Figure 1 displays the pairing gap $\Delta(k_F, k_F)$ in symmetric

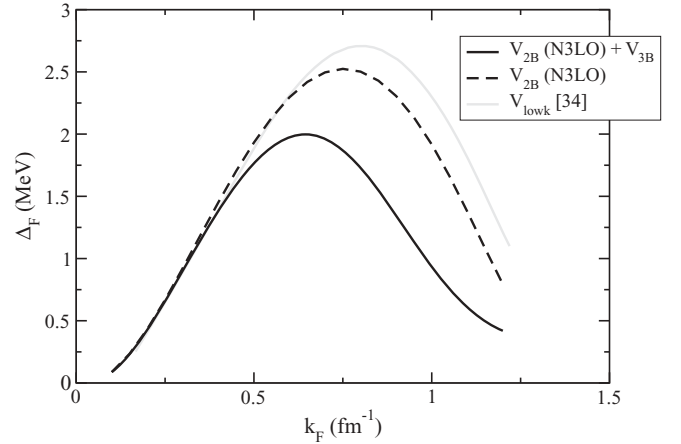


FIG. 1. Pairing gaps in symmetric nuclear matter in the 1S_0 channel as functions of the Fermi momentum. The dashed curve is obtained by including only the two-body (V_{2B}) chiral interaction, whereas the solid curve also includes the contribution of three-body (V_{3B}) forces. The gaps are compared to those obtained in Ref. [34] using the V_{lowk} potential.

nuclear matter as function of the Fermi momentum k_F . We plot results of the complete calculation that include two and three-body forces (solid curve) and the pairing gap obtained with only the two-body NN potential at $N^3\text{LO}$ (dashed curve). Our results are shown in comparison with those obtained in Ref. [34] using the V_{lowk} potential (with single-particle energies computed in Brueckner-Hartree-Fock theory).

III. MAPPING PROCEDURE

To implement the chiral NN potential at $N^3\text{LO}$ in the pairing channel of the RHB framework for finite nuclei, we adopt the approach introduced by Duguet [23] and later adopted by Tian *et al.* [24,25]. In nuclear matter the matrix element of the pairing force is approximated by an expression separable in momentum space:

$$\langle \mathbf{k} | V^{^1S_0} | \mathbf{k}' \rangle = -Gp(k)p(k'), \quad (4)$$

where \mathbf{k} and \mathbf{k}' are the relative momenta of the pair. By assuming a simple Gaussian ansatz $p(k) = e^{-a^2 k^2}$, in Ref. [23] the two parameters G and a were adjusted to reproduce the density dependence of the pairing gap in infinite matter at the Fermi surface, as calculated with the AV18 NN interaction [33]. The same fitting procedure was adopted in Ref. [24] to adjust the parameters of the Gaussian function to the pairing gap in nuclear matter computed with a Gogny force. For the D1S parameterization [9] of the Gogny force, $G = 728 \text{ MeV fm}^3$ and $a = 0.644 \text{ fm}$. Here we apply the same procedure to the chiral NN potential at the $N^3\text{LO}$ order. For finite nuclei, when the pairing force Eq. (4) is transformed

¹In Ref. [30] the two-body interaction comprises long-range one- and two-pion exchange contributions and a set of contact terms contributing up to fourth power in momenta ($N^3\text{LOW}$ potential developed lowering the cutoff scale to $\Lambda = 414 \text{ MeV}$). In addition, the authors employ the leading order chiral three-nucleon interaction with the corresponding parameters c_E , c_D , and $c_{1,3,4}$ adjusted in

calculations of few-body systems. Even though the results are in good agreement with previous calculations [31], one should note that higher order corrections could have non-negligible effects [32].

from momentum to coordinate space, it takes the form

$$V(\mathbf{r}_1, \mathbf{r}_2, \mathbf{r}'_1, \mathbf{r}'_2) = G\delta(\mathbf{R} - \mathbf{R}')P(r)P(r')\frac{1}{2}(1 - P^\sigma), \quad (5)$$

where $\mathbf{R} = \frac{1}{2}(\mathbf{r}_1 + \mathbf{r}_2)$ and $\mathbf{r} = \mathbf{r}_1 - \mathbf{r}_2$ denote the center of mass and the relative coordinates, $P(r)$ is the Fourier transform of $p(k)$,

$$P(r) = \frac{1}{(4\pi a^2)^{3/2}} e^{-r^2/4a^2}, \quad (6)$$

and the factor $1/2(1 - P^\sigma)$ projects on the 1S_0 channel. The pairing force has a finite range and, because of the presence of the factor $\delta(\mathbf{R} - \mathbf{R}')$, it preserves translational invariance. Even though $\delta(\mathbf{R} - \mathbf{R}')$ implies that this force is not completely separable in coordinate space, the corresponding antisymmetrized pp matrix elements can be represented as a sum of a finite number of separable terms, using a method developed by Talmi and Moshinsky. Using a Moshinsky-type expansion, the pairing interaction separable in momentum space was first employed in systematic nonrelativistic HFB calculations of pairing gaps in semimagic nuclei across the nuclear chart in Refs. [10,11]. When the nucleon wave functions are expanded in a harmonic oscillator basis [24,25], spherical or deformed, the sum converges relatively quickly. A relatively small number of separable terms reproduces with high accuracy the result of a calculation performed in the complete basis.

The parameters of the separable pairing force take the values $G = 892.0 \text{ MeV fm}^3$ and $a = 0.74 \text{ fm}$ for the N³LO potential and $G = 1045.0 \text{ MeV fm}^3$ and $a = 0.86 \text{ fm}$ for the complete potential $V(p, k)$. Recently a similar approach was employed in Refs. [11,14], where a low-rank separable representation was used to reproduce directly V_{lowk} and V_{3N} in the 1S_0 channel (for V_{3N} the density dependence was parametrized by a polynomial in the Fermi momentum). We note that in our case a single-Gaussian ansatz without explicit density dependence cannot perfectly reproduce the higher density behavior of the $V_{2B}(\text{N}^3\text{LO}) + V_{3B}$ pairing gap in symmetric nuclear matter. A slightly better agreement can be obtained by using a linear combination of three Gaussians with different widths and amplitudes for $p(k)$, as suggested in Ref. [24]. In Sec. IV we discuss the relevance of this issue, showing an explicit comparison between calculations employing respectively a single-Gaussian or a three-Gaussians ansatz.

IV. RESULTS FOR FINITE NUCLEI

The first study of pairing in finite nuclei with 3N forces was recently reported in Ref. [14]. Systematic calculations were performed for the odd-even mass staggering generated using a microscopic pairing interaction at first order in chiral low-momentum interactions. Significant repulsive contributions from the leading chiral 3N forces were found, and it was shown that combined two- and three-nucleon interactions account for approximately 70% of the empirical pairing gaps.

In the present analysis, employing the RHB model with the FKVW functional in the ph channel and the separable pairing force Eq. (5) in the pp channel, we have calculated the

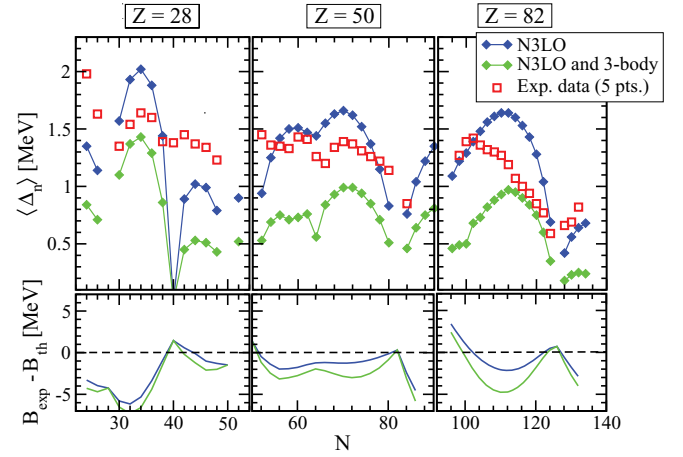


FIG. 2. (Color online) Theoretical average neutron pairing gaps (7) of the even-even isotopes of nickel $Z = 28$, tin $Z = 50$, and lead $Z = 82$, compared to the empirical values calculated from experimental masses using Eq. (8) (upper panel). Absolute deviations of the calculated binding energies from the experimental values [35] (lower panel).

self-consistent ground-state solutions for several sequences of isotopes (nickel, tin, and lead) and isotones ($N = 28$, $N = 50$ and $N = 82$). The total binding energies and average pairing gaps are compared to available data in Figs. 2 and 3. The experimental masses are from Ref. [35], and the average proton and neutron gaps [36]

$$\bar{\Delta} = \frac{\sum_k \Delta_k u_k v_k}{\sum_k v_k u_k} \quad (7)$$

are compared to empirical values determined using the five-point formula [37] for even-even nuclei:

$$\Delta^{(5)}(N_0) = -\frac{1}{8}[E(N_0 + 2) - 4E(N_0 + 1) + 6E(N_0) - 4E(N_0 - 1) + E(N_0 - 2)]. \quad (8)$$

$E(N_0)$ denotes the experimental binding energy of a nucleus with N_0 neutrons (Z_0 for protons). In Eq. (7) the sum is over proton or neutron canonical states, Δ_k is the diagonal matrix

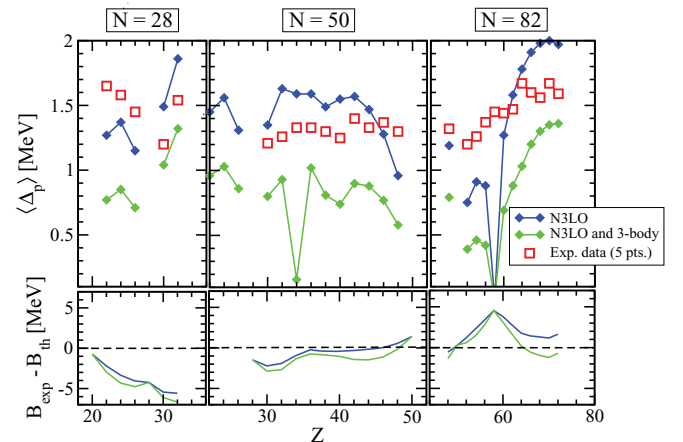


FIG. 3. (Color online) Same as described in the caption to Fig. 2 but for the chains of isotones $N = 28$, $N = 50$, and $N = 82$.

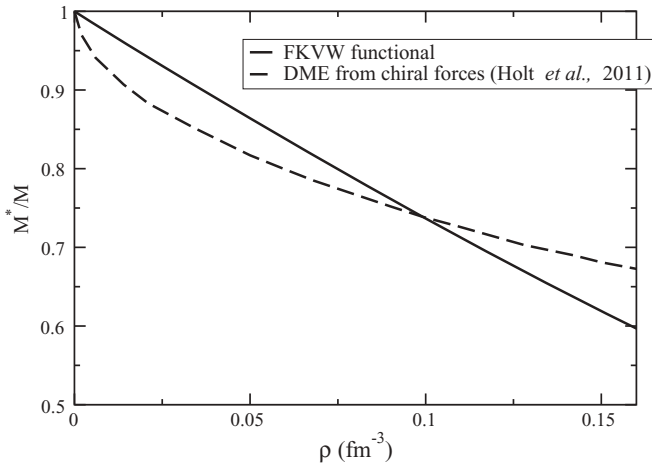


FIG. 4. M^*/M as function of the baryon density ρ employed in the FKVV functional (solid) [6], and the effective mass derived by Holt *et al.* [30] from microscopic chiral two- and three-nucleon interactions using a density-matrix expansion.

element of the pairing field in the canonical state k , and v_k denotes the corresponding eigenvalue of the one-body density matrix (occupation factor).²

The theoretical gaps shown in Figs. 2 and 3 have been calculated using the values of the parameters G and a that correspond to the nuclear matter pairing gaps in Fig. 1. The gaps calculated by including only the interaction V_{2B} (blue diamonds) reproduce on a quantitative level the isotopic and isotonic trends of the empirical gaps. Including the three-nucleon interaction V_{3B} induces a sizable reduction of the calculated gaps (green diamonds), in agreement with the results reported in Ref. [14]. The calculated gaps for the isotopic chains $Z = 28$, $Z = 50$, and $Z = 82$ indicate that missing higher order contributions (e.g., particle-vibration coupling) could play an important role [38,39]. Figure 3 displays similar results for the proton pairing gaps of the isotonic chains $N = 28$, $N = 50$, and $N = 82$ (we note that here the contribution of the Coulomb interaction in the pairing channel is neglected). The subshell closures that appear at $N = 40$ in the nickel chain [40], and at $Z = 58$ in the $N = 82$ chain [41], lead to a strong reduction of pairing correlations in the corresponding ground states.

A quantitative interpretation of the results of this work must take into account at least two additional effects. First, the effective mass employed in Eq. (3) is not exactly identical to the one that is used in the ph functional (at leading order in the nonrelativistic expansion). In the latter case the dominant contribution is generated by the *condensates* (solid curve in Fig. 4), and this leads to a nearly linear density dependence of the effective mass. The same contribution is present in Holt's

²This choice for the pairing gaps is, of course, not unique. In Ref. [12], for instance, the theoretical gap Δ_{LCS} (lowest canonical state) corresponds to the diagonal pairing matrix element Δ_i in the canonical single-particle state ϕ_i whose quasiparticle energy is the lowest, whereas empirical gaps are computed from binding energies using three-point mass differences centered on odd-mass nuclei.

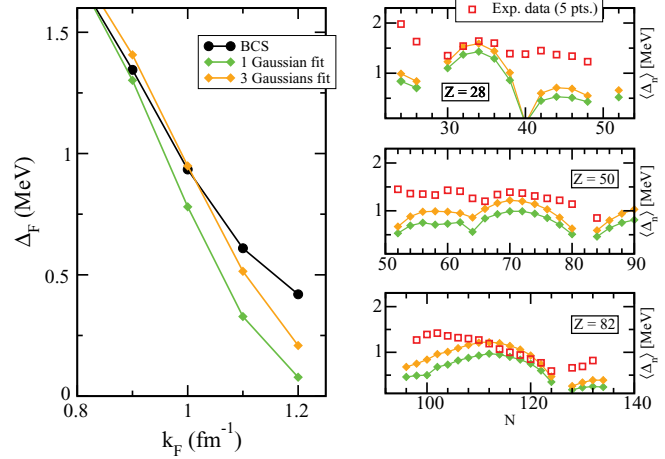


FIG. 5. (Color online) Right panel: High-density behavior of the 1S_0 pairing gap in symmetric nuclear matter obtained from V_{2B} and V_{3B} forces (black circles), in comparison with gaps calculated using a single-Gaussian (green [light gray] diamonds) ansatz and a linear combination of three Gaussians (orange [dark gray] diamonds) for the separable interaction introduced in Sec. III. For smaller values of the Fermi momentum the differences are negligible. Left panel: Average neutron pairing gaps Eq. (7) for the even-even isotopes of nickel, tin, and lead, calculated with a single-Gaussian ansatz (green [light gray] diamonds) and a three-Gaussians ansatz (orange [dark gray] diamonds) for the separable pairing force, in comparison with empirical values (red squares).

calculation [30] but within a more consistent framework that, at present, is not applicable to finite nuclei. In this case the behavior of the effective mass as function of the baryon density is slightly different (dashed curve in Fig. 4). In the future this inconsistency can be cured by improving the FKVV density functional for finite nuclei.

The second issue is that the simple choice of a single-Gaussian ansatz introduced in Sec. III cannot perfectly reproduce the high-density behavior of the pairing gap $\Delta(k_F, k_F)$. By using a more complex ansatz, that is, a linear combination of three Gaussians as suggested in Ref. [24], the agreement with the $V_{2B}(N^3\text{LO}) + V_{3B}$ pairing gap in nuclear matter can be improved, and in finite nuclei this leads to an increase of the pairing gaps by 20% to 30% (cf. Fig. 5 for the isotopic chains).

The exact values of the pairing gaps, of course, are also affected by the choice of the functional in the ph channel, as it determines the spectrum of single-nucleon states. In Ref. [42] we tested the separable pairing interaction Eq. (4) in calculations of pairing gaps, using different relativistic point-coupling functionals. The sizable reduction produced by V_{3B} is, of course, preserved even if in some cases one finds an unrealistic collapse of pairing correlations caused by large gaps in the single-particle spectra. The present results are in qualitative agreement with those obtained in Ref. [14]. On the quantitative level it is difficult to disentangle the differences that arise from the different choice of EDFs in the ph channel from effects caused by the different treatment of the density dependence of the averaged NNN interaction. A more detailed comparison of the two approaches is planned for a forthcoming publication.

The influence of three-body forces on the total binding energy is much less pronounced, as shown in the lower panels of Figs. 2 and 3, where we display the absolute deviations of the calculated binding energies from the experimental values. On the one hand this is because pairing correlations contribute much less than the mean-field self-energies to the total binding. On the other hand this is a well-known characteristic of a self-consistent calculation in that, for a given nucleus, a reduction of pairing results in an effective enhancement of the mean-field contribution to the total energy and vice versa. In general, the combination of the FKVW ph effective interaction and the separable pairing force Eq. (5) produces results for the total binding energies that are comparable to those obtained with the best empirical nonrelativistic and relativistic energy density functionals. For the nickel isotopes the largest deviations are in the region $Z \approx N$, where one expects additional contributions from proton-neutron correlations that are not included explicitly in the FKVW functional. In the tin isotopes the calculated masses start deviating from data in neutron-rich nuclei beyond the major shell closure at $N = 82$, whereas for lead nuclei the deviations are most pronounced in the lightest, neutron-deficient isotopes that are characterized by soft potentials and shape coexistence.

V. CONCLUSIONS

A consistent microscopic approach to the structure of open-shell nuclei has been introduced, in which both the ph and the pp channels of the effective nuclear interaction are fully

determined by chiral pion-nucleon dynamics. By employing an ansatz for the pairing force that is separable in momentum space, we have performed an efficient mapping of the chiral potential in the pairing channel (at the N^3LO and N^2LO orders in the two-body and three-body sectors, respectively) to an effective pp interaction for finite nuclei. The two parameters of the separable pairing force are adjusted to reproduce the density dependence of the pairing gaps in symmetric nuclear matter. The resulting effective pairing interaction thus enables, on the one hand, the treatment of pairing correlations in finite nuclei using pairing functionals constrained by chiral dynamics and, on the other hand, calculations in the pp channel with a finite-range interaction. The significant advantage is that the computational cost is greatly reduced when compared to nonlocal finite-range forces like, for instance, the empirical Gogny force. A noteworthy result of the present investigation is that it confirms the important role of three-body forces in determining pairing gaps in finite nuclei. Additional effects that could play a role in determining pairing gaps in finite nuclei need to be further explored.

ACKNOWLEDGMENTS

This work was partly supported by INFN, MIUR, and MZOS (Project No. 1191005-1010). We acknowledge useful discussions with N. Kaiser, W. Weise, and E. Vigezzi and thank J. W. Holt for providing numerical values for the three-body potential.

-
- [1] M. Bender, P. H. Heenen, and P. G. Reinhard, *Rev. Mod. Phys.* **75**, 121 (2003).
 - [2] J. Dobaczewski, *J. Phys. G* **37**, 060301 (2010).
 - [3] R. M. Dreizler and E. K. U. Gross, *Density Functional Theory* (Springer, Berlin, 1990); E. Engel and R. M. Dreizler, *Density Functional Theory: An Advanced Course* (Springer, Berlin, 2011).
 - [4] P. Finelli, N. Kaiser, D. Vretenar, and W. Weise, *Eur. Phys. J. A* **17**, 573 (2003).
 - [5] P. Finelli, N. Kaiser, D. Vretenar, and W. Weise, *Nucl. Phys. A* **735**, 449 (2004).
 - [6] P. Finelli, N. Kaiser, D. Vretenar, and W. Weise, *Nucl. Phys. A* **770**, 1 (2006).
 - [7] S. Fritsch, N. Kaiser, and W. Weise, *Nucl. Phys. A* **750**, 259 (2005).
 - [8] D. Vretenar, A. V. Afanasjev, G. A. Lalazissis, and P. Ring, *Phys. Rep.* **409**, 101 (2005).
 - [9] J. F. Berger, M. Girod, and D. Gogny, *Comput. Phys. Commun.* **63**, 365 (1991).
 - [10] T. Duguet and T. Lesinski, *Eur. Phys. J. St.* **156**, 207 (2008).
 - [11] T. Lesinski, T. Duguet, K. Bennaceur, and J. Meyer, *Eur. Phys. J. A* **40**, 121 (2009).
 - [12] K. Hebeler, T. Duguet, T. Lesinski, and A. Schwenk, *Phys. Rev. C* **80**, 044321 (2009).
 - [13] T. Duguet, T. Lesinski, K. Hebeler, and A. Schwenk, *Mod. Phys. Lett. A* **25**, 1989 (2010).
 - [14] T. Lesinski, K. Hebeler, T. Duguet, and A. Schwenk, *J. Phys. G* **39**, 015108 (2012).
 - [15] N. Kaiser, T. Nikšić, and D. Vretenar, *Eur. Phys. J. A* **25**, 257 (2005).
 - [16] R. Machleidt and D. R. Entem, *Phys. Rep.* **503**, 1 (2011).
 - [17] E. Epelbaum, H.-W. Hammer, and U.-G. Meissner, *Rev. Mod. Phys.* **81**, 1773 (2009).
 - [18] J. W. Holt, N. Kaiser, and W. Weise, *Phys. Rev. C* **81**, 024002 (2010).
 - [19] K. Hebeler and A. Schwenk, *Phys. Rev. C* **82**, 014314 (2010).
 - [20] K. Hebeler, S. K. Bogner, R. J. Furnstahl, A. Nogga, and A. Schwenk, *Phys. Rev. C* **83**, 031301 (2011).
 - [21] S. Gandolfi, A. Y. Illarionov, K. E. Schmidt, F. Pederiva, and S. Fantoni, *Phys. Rev. C* **79**, 054005 (2009).
 - [22] A. Lovato, O. Benhar, S. Fantoni, A. Y. Illarionov, and K. E. Schmidt, *Phys. Rev. C* **83**, 054003 (2011).
 - [23] T. Duguet, *Phys. Rev. C* **69**, 054317 (2004).
 - [24] Y. Tian, Z. Y. Ma, and P. Ring, *Phys. Lett. B* **676**, 44 (2009).
 - [25] Y. Tian, Z. Y. Ma, and P. Ring, *Phys. Rev. C* **80**, 024313 (2009).
 - [26] A. B. Migdal, *Theory of Finite Fermi Systems and Applications to Atomic Nuclei* (Interscience, New York, 1967).
 - [27] D. J. Dean and M. Hjorth-Jensen, *Rev. Mod. Phys.* **75**, 607 (2003), and references therein.
 - [28] H. J. Schulze, J. Cugnon, A. Lejeune, M. Baldo, and U. Lombardo, *Phys. Lett. B* **375**, 1 (1996).
 - [29] U. Lombardo, H. Schulze, C.-W. Shen, and W. Zuo, *Int. J. Mod. Phys. E* **14**, 513 (2005).
 - [30] J. W. Holt, N. Kaiser, and W. Weise, *Eur. Phys. J. A* **47**, 128 (2011).

- [31] S. Fritsch, N. Kaiser, and W. Weise, *Nucl. Phys. A* **750**, 259 (2005).
- [32] J. W. Holt, N. Kaiser, and W. Weise, *Nucl. Phys. A* **870-871**, 1 (2011).
- [33] R. B. Wiringa, V. G. J. Stoks, and R. Schiavilla, *Phys. Rev. C* **51**, 38 (1995).
- [34] A. Sedrakian, T. T. S. Kuo, H. Muther, and P. Schuck, *Phys. Lett. B* **576**, 68 (2003).
- [35] G. Audi, A. H. Wapstra, and C. Thibault, *Nucl. Phys. A* **729**, 337 (2003).
- [36] M. Bender, K. Rutz, P. G. Reinhard, and J. A. Maruhn, *Eur. Phys. J. A* **8**, 59 (2000).
- [37] P. Moller and J. R. Nix, *Nucl. Phys. A* **536**, 20 (1992).
- [38] F. Barranco, P. F. Bortignon, R. A. Broglia, G. Colo, P. Schuck, E. Vigezzi, and X. Vinas, *Phys. Rev. C* **72**, 054314 (2005).
- [39] G. Gori, F. Ramponi, F. Barranco, P. F. Bortignon, R. A. Broglia, G. Colo', and E. Vigezzi, *Phys. Rev. C* **72**, 011302 (2005).
- [40] R. Broda, B. Fornal, W. Krolas, T. Pawlat, D. Bazzacco, S. Lunardi, C. Rossi-Alvarez, R. Menegazzo *et al.*, *Phys. Rev. Lett.* **74**, 868 (1995).
- [41] W. H. Long, H. Sagawa, J. Meng, and N. Van Giai, *Europhys. Lett.* **82**, 12001 (2008).
- [42] P. Finelli, *Nuclear Pairing from Chiral Pion-Nucleon Dynamics*, Prog. Theor. Phys. Suppl., Proceedings of YKIS2011 Workshop, Kyoto.